Model Identification by Periodic-Orbit Analysis for NMR-Laser Chaos

L. Flepp, R. Holzner, and E. Brun
Physik-Institut der Universität, CH-8001 Zürich, Switzerland

M. Finardi and R. Badii
Paul-Scherrer Institut, CH-5232 Villigen, Switzerland
(Received 2 May 1991)

It is shown that the conventional Bloch-Kirchhoff description of NMR-laser activity needs the inclusion of a nonlinear relaxation term for the transverse magnetization in order to account for the experimental observation. The validity of the modified equations is demonstrated by comparing in a two-parameter space the Poincaré sections and periodic-orbit structures of model and experiment. All unstable orbits up to order nine have been extracted and employed to obtain an approximation to a generating partition.

PACS numbers: 05.45.+b, 76.60.−k

In this Letter, we present a detailed analysis of high-quality (i.e., low-noise, drift-free, long) time series from an NMR-laser system with modulated parameters and propose an extension of the conventional Bloch-Kirchhoff description which yields very good quantitative agreement with the experimental observation. We investigated the bifurcation structure of the system in a two-parameter space, constructed Poincaré sections, and extracted all unstable periodic orbits up to order nine. This allowed us to demonstrate the validity of the extended Bloch-type equations and evaluate the topological entropy K_0 by means of explicit construction of the symbolic dynamics directly from the embedded time series.

The NMR-laser [1] activity is provided by the nuclear spins of the ^{27}Al in a ruby crystal, placed at a temperature of 4.2 K in a static magnetic field $\mathbf{B}_0$ of magnitude 1.1 T. The total nuclear magnetization $\mathbf{M}=(M_x,M_y,M_z)$ precesses with the NMR frequency $\nu_a=12.3$ MHz. The population inversion is obtained by means of a microwave pump (dynamic nuclear polarization) [1] and the resonance by enclosing the active medium in a cavity: in our case an LC circuit, tuned to ν_a for single-mode selection, which provides the feedback radiation field $\mathbf{B}$ (proportional to the current in the circuit) necessary for coherent spin-flip behavior. Furthermore, the cavity is forced to operate with a modulated quality factor $Q(t)=Q_0(1+A\cos\Omega t)$, where $\Omega\in(350,800)$ s^{-1} and $A\in(0,0.03)$. The "laser output" is proportional to the transverse nuclear-magnetization amplitude $M_t=(M_x^2+M_y^2)^{1/2}$.

The extended Bloch-type laser (EBL) model in the rotating-frame approximation [2] reads

$$\dot{x}=\sigma[y-x/f(\tau)],$$
$$\dot{y}=-y(1+ay)+rx-xz, \qquad (1)$$
$$\dot{z}=-bz+xy,$$

where $x\propto B_t$, $y\propto M_t\geq 0$, $z\propto M_z-M_e$: B_t represents the rotating field amplitude and M_e the pump magnetization. The proportionality factors, as well as the parameters $\sigma=4.875$, $r=1.807\propto M_e$, and $b=2\times10^{-4}$, depend on various physical constants [2]. The function $f(\tau)=1+A\cos(\omega\tau)$ describes the modulation with frequency $\omega\in(0.014,0.034)$ and τ is a rescaled time. Equations (1) reduce to the Lorenz system [3] for $a=A=0$. Under these conditions, the asymptotic attractor is the fixed point $x=y=x^*=[b(r-1)]^{1/2}$, $z=z^*=r-1$.

The difference with the conventional model consists of the term $-ay^2$, where $a\approx0.2621$, which describes a nonlinear damping for the transverse magnetization y (recall that $y\geq0$). This term is essentially the first nonlinear contribution in a series expansion [4] and has been introduced to account for the observed decay of the laser output (relaxation oscillation) to a stable fixed point in the absence of the modulation ($A=0$), after Q switching. The corresponding time evolution of $y(t)$ vs t is displayed in Fig. 1 for both experiment [Fig. 1(a)] and model [Fig. 1(b)]: In the latter case, we also marked the position of the peaks (circles) and indicated (dashed line) the envelope of the damped oscillation obtained from the conventional model ($a=0$). The manifest discrepancy is not surprising, since the phenomenological Bloch equations often provide incorrect predictions in solids [5]. It must be stressed that the correction term is actually very small: In fact, by setting $(X,Y,Z)=(x/x^*,y/x^*,(z-z^*)/x^*)$ and rescaling time τ to $\tau'=\tau x^*$, we obtain the term $-Y(1+a'Y)/x^*$, where $a'=3.33\times10^{-3}$ and $Y\in(0,3)$ for all considered A values. This transformation also shows that X can be adiabatically eliminated, since $\sigma\rightarrow\sigma'\approx384\gg1$, so that $X\approx Yf(\tau')$ and Y never changes sign [4].

The study of the transient behavior after Q switching provides a first confirmation of the validity of our approach, although limited to a short time interval (0.2 s) and to a single-parameter choice. In order to extend our analysis to generic asymptotic motion, we considered the Q-modulated laser which can exhibit chaotic behavior [6]. The correspondence between model and experiment

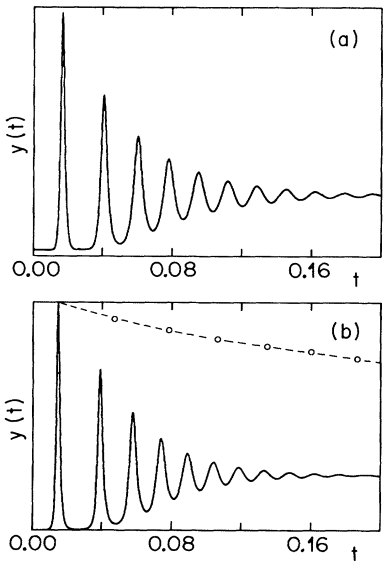

FIG. 1. Time evolution for the transverse magnetization $y(t)$ (in arbitrary units) vs time t (in s), after Q switching: (a) experiment; (b) EBL model. The circles represent the peaks of the corresponding curve (the dashed line is its envelope) obtained from the conventional model: In this case, both decay rate and relaxation frequency are incorrectly reproduced.

is shown by performing a sequence of increasingly more stringent tests: comparison between bifurcation diagrams, stability regions in the ω-A parameter space, Poincaré sections, and sets of unstable periodic orbits.

The phenomenology of the EBL system (1) can be discussed with reference to Fig. 2 [7], where the ω-A parameter space is displayed. Various domains of stable periodic behavior are shown for both experiment [Fig. 2(a)] and model [Fig. 2(b)]. The two pictures are in very good agreement to within the effect of experimental noise, which destroys thin stability regions in 2(a). The finiteness of the measurement resolution for the parameter values (2 or 3 digits) also contributes to the uncertainty of the comparison: The period-5 stable orbit visible in 2(a), for example, has been detected only as unstable in 2(b). The conventional Bloch-Kirchhoff equations, on the other hand, exhibit a behavior which is only qualitatively similar to that shown in Fig. 2 [6].

Several bifurcation diagrams for the variable y have been experimentally recorded as a function of A, at different ω values. The accuracy of model (1) has been confirmed in the whole parameter range shown in Fig. 2 by comparison with the numerical results. Five crisis lines [8] have been detected in the chaotic region where the strange attractors collide with different unstable periodic orbits.

A more severe test for the EBL equations has been performed by studying chaotic attractors for various parameter values, both in the full embedding space and on Poincaré sections [9]. Scalar time series $\{\xi_1,\xi_2,\ldots,\xi_N\}$, consisting of $N=8\times10^5$ twelve-bit integers, have been recorded by sampling the transverse magnetization $M_t(t)$ with a frequency $\nu=25/T$, where $T=2\pi/\Omega$ is the period of the forcing term: i.e., $\xi_i=M_t(i/\nu)$. The data are then embedded in an E-dimensional space by constructing vectors of the form $\mathbf{v}_k=\{\xi_k,\xi_{k+5},\ldots,\xi_{k+5(E-1)}\}$, where $5/\nu$ is the appropriate delay time [9]. Portions of trajectory which lie close to the unstable periodic orbits of the system have then been identified by requiring them to return in certain (spherical) regions of radius R within selected time intervals (chosen around multiplets of T, up to $9T$). The precision R with which the detected recurrent orbits shadow the actually periodic ones has been chosen to vary with the position in phase space, in order to minimize the relative error in the search. Further-

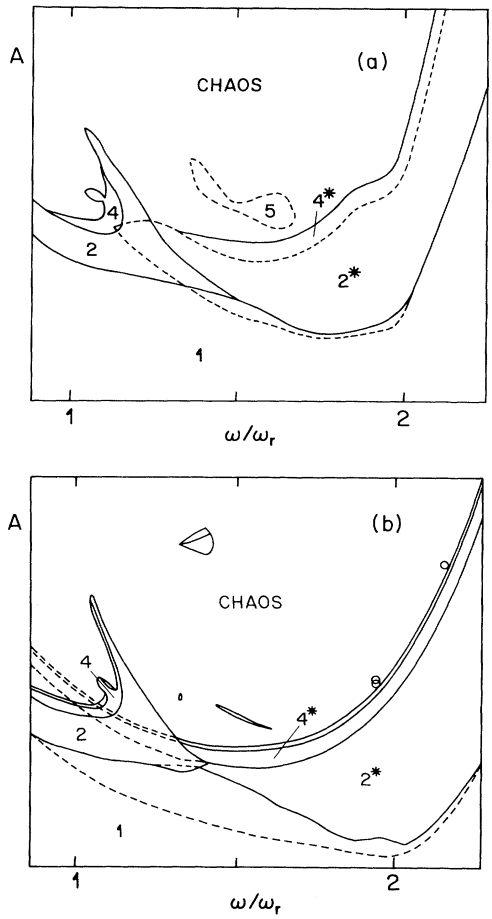

FIG. 2. Regions of existence of the main stable periodic orbits for the NMR-laser system in the parameter space ω-A: (a) experiment; (b) EBL model. The frequency is reported in units of the rescaled relaxation frequency $\omega_r=0.0163$. Two different periods two and four (marked as 2,2* and 4,4*) coexist. Multistability regions are delimited by dashed lines. The circles in (b) indicate the points (1.944,0.018), (1.944,0.0185), and (2.15,0.027) at which the periodic-orbit analysis has been carried out.

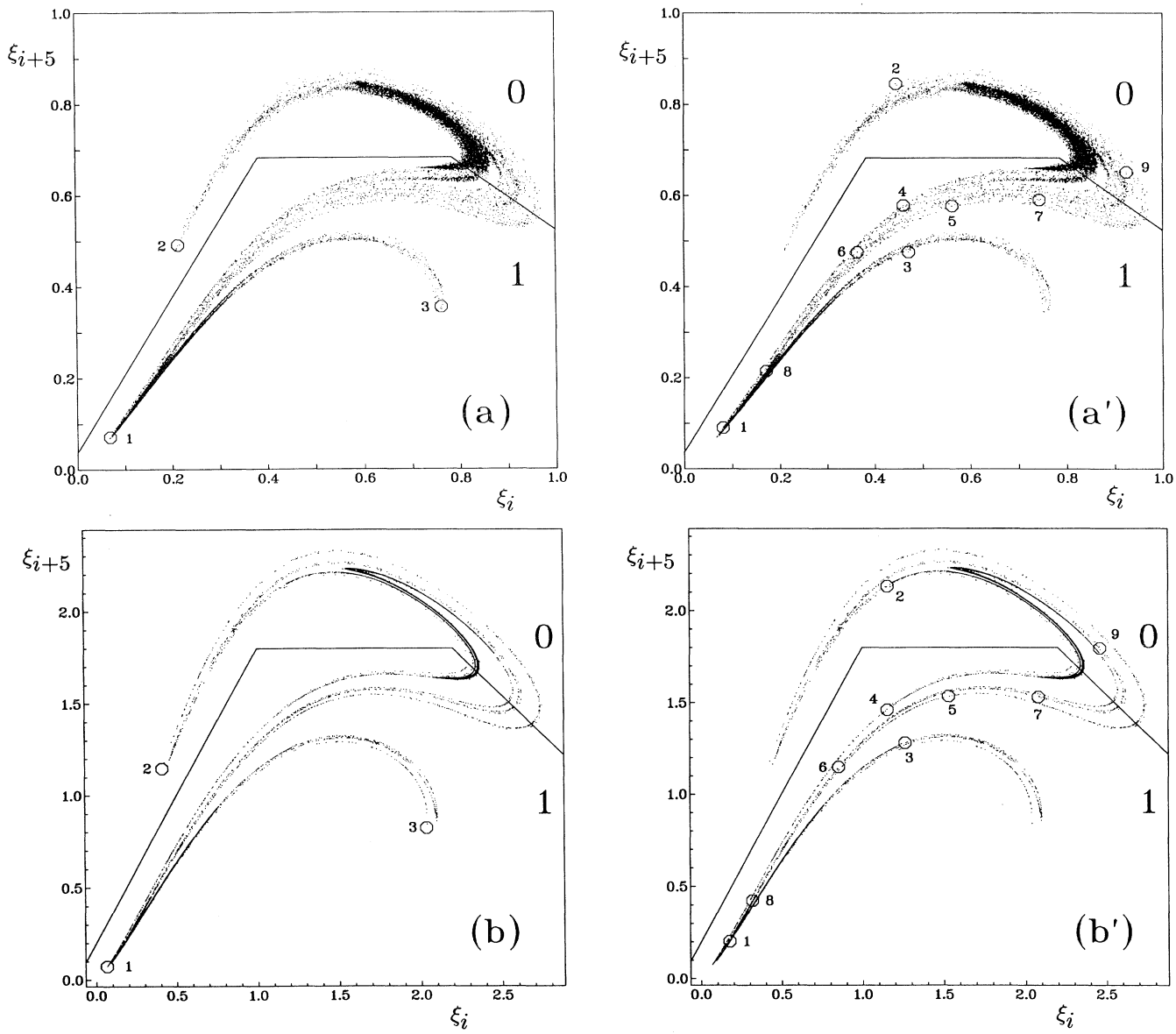

FIG. 3. Two-dimensional projections of the Poincaré section for $A=0.018$ and $\omega=0.031\,68$, and binary partition with elements labeled 0 and 1. The intersection points of the (a),(b) period-3 and of the (a'),(b') period-9 cycle are labeled in order of occurrence: (a) experiment; (b) model.

more, R is proportional to $\sqrt{E}$ and independent of the sampling time $1/\nu$, so that the results are consistent throughout the physically meaningful variation range [9] for E and ν. A Newton method has been used to locate the periodic orbits of the differential model (1). All cycles up to order nine have been compared with the experimental ones and found to agree very well in embedding spaces of dimension E between 6 and 16. In fact, the information dimension D_1 [9] for all considered strange attractors (the corresponding parameter values are indicated by circles in Fig. 2) is between 2.1 and 2.4 [10], so that $2D_1+1<6$.

In order to obtain a more complete characterization of the dynamics, we have constructed Poincaré sections Σ by considering embedded points $\mathbf{v}_k$ which lie 25 time units apart from each other (the system is, in fact, externally forced). The intersection points of the unstable cycles with Σ have then been assigned a different symbolic labeling through a binary partition [9] $\mathcal{D}=\{\Delta_0,\Delta_1\}$. Recall that a generating partition associates a unique phase-space point to each infinitely long symbolic sequence (among which are the periodic ones). Hence, the partition $\mathcal{D}$ constitutes a good approximation to a generating one, since it distinguishes all periodic points up to order

nine [11,12(b),12(c)]. Of course, separating periodic points is a necessary (although not, in general, sufficient) condition for $\mathcal{D}$ to be generating. In Fig. 3, we report experimental [3(a) and 3(a')] and numerical [3(b) and 3(b')] strange attractors on a two-dimensional projection of the Poincaré section Σ for $A=0.018$ and $\omega=0.031\,68$, together with the curve defining $\mathcal{D}$. Notice the intersection points of a period-3 orbit [3(a) and 3(b)] and of a period-9 orbit [3(a') and 3(b')] with Σ. The former one lies "on the border" of the attractor and gives rise to a crisis for $A_c \approx 0.018\,02$.

The analysis of the symbolic dynamics, performed with the unfolding method of Ref. [12], leads to a description in terms of a full binary tree over the two primitive words $w_1=1$, $w_2=01$ for both experiment and model up to hierarchical level 4 (the longest orbit of which is 01010101). In fact, the only experimental forbidden sequence is 00, whereas numerical calculations show that also three strings of length 9 are not allowed. The topological entropy is therefore approximated by $K_0=0.481 = \ln[(1+\sqrt{5})/2]$ [12(b)] at the experimental resolution. The prime cycles [13] have the following encodings: w_1, w_2, w_2w_1, $w_2w_1^2$, $w_2^2w_1$, $w_2w_1^3$, $w_2^2w_1^2$, $w_2w_1^4$, $w_2^2w_1^3$, $w_2w_1^5$, $w_2^3w_1^2$, $w_2^2w_1^4$, $w_2w_1^6$, $w_2^2w_1^5$, and $w_2w_1^7$, where w^n denotes the nth repetition of word w. The logic-tree representation of the symbolic dynamics constitutes an invariant topological characterization of the system. The full coincidence found between measured and numerical data (confirmed for the other two time series) clearly shows that the EBL model indeed describes the experimental observation up to the available resolution. A more complete characterization of the dynamics, which includes metric invariants as well (sequence probabilities, scaling functions, thermodynamic averages [13], and complexity [12]), will be presented elsewhere [4].

We acknowledge useful discussions with F. Waldner, P. F. Meier, and P. Talkner and financial support by the Swiss National Science Foundation.

[1] P. Boesiger, E. Brun, and D. Meier, Phys. Rev. Lett. **38**, 602 (1977).
[2] E. Brun, B. Derighetti, D. Meier, R. Holzner, and M. Ravani, J. Opt. Soc. Am. B **2**, 156 (1985).
[3] E. N. Lorenz, J. Atmos. Sci. **20**, 130 (1963).
[4] A more detailed discussion is presented in L. Flepp, R. Holzner, E. Brun, M. Finardi, and R. Badii (to be published).
[5] A. Abragam, *Principles of Nuclear Magnetism* (Clarendon, Oxford, 1989).
[6] M. Ravani, B. Derighetti, E. Brun, G. Broggi, and R. Badii, J. Opt. Soc. Am. B **5**, 1029 (1988).
[7] The rescaled equations for (X,Y,Z) have been actually integrated.
[8] C. Grebogi, E. Ott, and J. A. Yorke, Phys. Rev. Lett. **48**, 1507 (1982).
[9] J.-P. Eckmann and D. Ruelle, Rev. Mod. Phys. **57**, 617 (1985).
[10] They have been evaluated by means of the nearest-neighbor method; R. Badii and A. Politi, J. Stat. Phys. **40**, 725 (1984); G. Broggi, J. Opt. Soc. Am. B **5**, 1020 (1988).
[11] D. Auerbach, P. Cvitanović, J. P. Eckmann, G. Gunaratne, and I. Procaccia, Phys. Rev. Lett. **58**, 2387 (1987).
[12] (a) R. Badii, Europhys. Lett. **13**, 599 (1990); (b) R. Badii, M. Finardi, and G. Broggi, in *Chaos, Order and Patterns,* edited by P. Cvitanović *et al.* (Plenum, New York, 1991); (c) R. Badii, in *Measures of Complexity and Chaos,* edited by N. B. Abraham *et al.* (Plenum, New York, 1990).
[13] P. Cvitanović, Phys. Rev. Lett. **61**, 2729 (1988).